RSC Applied Interfaces

PAPER

View Article Online
View Journal | View Issue

Check for updates

Cite this: RSC Appl. Interfaces, 2026, 3, 192

Received 28th September 2025, Accepted 8th December 2025

DOI: 10.1039/d5lf00291e

rsc.li/RSCApplInter

Fabrication of low-fouling reverse osmosis membranes by grafting poly(2-methoxyethyl acrylate) *via* surface-initiated atom transfer radical polymerization method

Ines Haddar,[†a] Tomoki Kato,[a] Shin-ichi Nakao,[a] Xiao-lin Wang,[ac] Kazumi Tsukamoto,[b] Takahiro Kawakatsu[b] and Kazuki Akamatsu[*a]

The surfaces of polyamide-based low-pressure reverse osmosis (RO) membranes were modified with poly(2-methoxyethyl acrylate) (PMEA) *via* surface-initiated atom transfer radical polymerization for the first time to achieve low-fouling characteristics. The successful grafting of PMEA was demonstrated by attenuated total reflectance Fourier-transform infrared spectroscopy and zeta potential measurements. The grafting amount could be tuned from 0.020 to 0.23 mg cm^{-2} by changing the grafting time. The modified membranes maintained their salt rejection performances with slight reductions of pure water permeability especially when the grafting amount was smaller than 0.05 mg cm^{-2}. This result indicated that the grafted PMEA had almost no effect on salt rejection but slightly increased the permeation resistance. Compared with unmodified membranes, the modified membranes were found to exhibit low fouling against a variety of organic substances, such as lysozyme, guar gum and tetraethylene glycol monooctyl ether. The results indicate that surface modification of a low-pressure RO membrane with PMEA is a feasible method to obtain a membrane with low-fouling characteristics.

1. Introduction

The escalating global water crisis necessitates the urgent development of solutions to meet challenges arising from population growth, expanded agriculture, economic development and the looming threat of climate change.[1,2] The United Nations estimates that severe water scarcity will affect over 2.7 billion people by 2025, particularly in North African and Middle Eastern countries.[3] To address this crisis and reach sustainable development goals, unconventional water sources are being explored, where gold standard thin film composite (TFC) polyamide membranes are employed for various membrane technology applications.[4–6]

Reverse osmosis (RO) technology has emerged as a versatile and energy-efficient solution. This technology offers high flux together with high selectivity for several applications such as seawater desalination, ultrapure water production and wastewater treatment, which contributes to sustainability.[7,8] To date, most commercial TFC RO membranes are formed as flat sheets with an ultrathin aromatic polyamide film coating. The polyamide layer is formed by interfacial polymerization with amine monomers and acyl chloride monomers.[9,10] These membranes perform well and are already in widespread production. However, persistent fouling issues, influenced by factors such as the membrane material, zeta potential of the membrane surface, and operational conditions, pose considerable challenges.[11,12] Organic fouling remains a critical concern because of its detrimental impact on membrane performance and necessitates frequent chemical cleaning, which increases operational costs and decreases the membrane lifespan.[13] Major fouling substances include proteins, polysaccharides and surfactants.[14–17] One possible approach to assessing fouling behavior in both laboratory settings and practical operations involves the use of model substances, such as lysozyme for proteins, guar gum for polysaccharides and tetraethylene glycol monooctyl ether (TEGMO) for surfactants.

One effective strategy for mitigating membrane fouling has been to modify the membrane surface with hydrophilic

[a] Department of Environmental Chemistry and Chemical Engineering, School of Advanced Engineering, Kogakuin University, 2665-1 Nakano-machi, Hachioji-shi, Tokyo 192-0015, Japan. E-mail: akamatsu@cc.kogakuin.ac.jp; Tel: +81 42 628 4584
[b] Kurita Innovation Hub, Kurita Water Industries Ltd., 1-4-1 Daikanyama, Akishima-shi, Tokyo 196-0005, Japan
[c] Department of Chemical Engineering, Tsinghua University, Beijing 100084, People's Republic of China
† Kurita Water Industries Ltd., Kurita Innovation Hub, 1-4-1 Daikanyama, Akishima-shi, Tokyo 196-0005, Japan.

polymers, either through physical deposition or covalent immobilization.[18–22] This approach appeared pivotal because it can prevent the hydrophobic interactions between the polyamide membrane and certain organic foulants that largely enable membrane fouling. Previous studies have highlighted the efficacy of specific polymers, such as poly[(2-methacryloyloxy)ethyl]dimethyl[3-sulfopropyl]ammonium hydroxide (pMEDSAH),[23] poly(carboxybetaine acrylic acetate)[24] and poly(2-methacryloyloxyethyl phosphorylcholine),[25] in preventing biofouling. Additionally, it has been demonstrated that poly(2-methoxyethyl acrylate) (PMEA) is an effective surface modifier for the fabrication of low-fouling microfiltration membranes.[26–28] Unlike other low-fouling polymers mentioned above, PMEA is insoluble in water. PMEA has been extensively investigated for use in biomaterials and has excellent biocompatibility. Tanaka *et al.* demonstrated that "intermediate water" can effectively prevent protein adsorption onto membrane surfaces.[29–31] At hydrated polymers, three types of water exist, "free water", "intermediate water" (*i.e.* freezing bound water) and "non-freezing water", which can be classified using differential scanning calorimetry. The strong correlation between the amount of the intermediate water and the blood compatibility of the biomaterial polymers were demonstrated.[32] Furthermore, Nagumo *et al.* demonstrated that the hydrated PMEA prohibits the adsorption of organic substances by using molecular dynamic simulations.[33] Based on these publications, PMEA is one of the potential polymers for surface modification to achieve low-fouling properties. Surface-initiated atom transfer radical polymerization (SI-ATRP) is a promising alternative to conventional modification methods.[34–36] Unlike techniques such as redox reactions and electrostatic coating, SI-ATRP offers precise control over the length of the grafted polymers, overcoming limitations such as low surface density and poor stability. This method holds considerable potential for advancing membrane technology, addressing key challenges and enhancing performance and longevity.

Our objective in this study was to fabricate low-fouling RO membranes with enhanced resistance against organic fouling by harnessing the benefits of grafted PMEA. To tailor the membrane properties precisely, we controlled the grafting amount through varying the polymerization time. The surface properties of the membranes were analyzed by attenuated total reflectance Fourier-transform infrared (ATR-FTIR) spectroscopy and zeta potential measurement. To demonstrate the effectiveness of our modified membranes in real-world scenarios, we conducted filtration and immersion tests using three different aqueous solutions containing lysozyme as a model protein-like foulant, guar gum as a model polysaccharide-like foulant and TEGMO as a model surfactant-like foulant. The meticulous control strategy enabled us to fine-tune the surface characteristics of the RO membrane and optimize the performance towards enhanced organic fouling resistance.

2. Experimental

2.1. Materials

As the base membrane, a polyamide-based low-pressure RO membrane, ES20, which was purchased from Nitto Denko Corporation, Japan, was used. Hexane, 3-aminopropyltrimethoxysilane, L(+)-ascorbic acid, tris(2-pyridylmethy)amine (TPMA), copper(II) bromide ($CuBr_2$), methanol, 2-methoxyethyl acrylate (MEA), sodium chloride (NaCl) and lysozyme were purchased from Fujifilm Wako Pure Chemical Corp., Japan. In addition, α-bromoisobutyryl bromide (BIBB) and TEGMO were purchased from Sigma-Aldrich and guar gum (F50, 5000 cps) was purchased from San-ei Yakuhin Boeki Co., Ltd., Japan. In some cases, microfiltration membranes whose average pore size was 60 nm were used to pretreat the feed solution to remove undissolved substances. The MEA monomer was distilled before use, whereas all other chemicals were used as received.

2.2. Surface modification *via* SI-ATRP

First, the RO membrane was pretreated using a procedure reported elsewhere.[23] Two wooden plates, each measuring 12 cm × 12 cm, and eight double clips were employed to securely hold the membrane during the process. A 1 vol% 3-aminopropyltrimethoxysilane aqueous solution was poured on the top surface of the RO membrane. After 10 min, the membrane surface was washed thoroughly with pure water. Second, a 3 wt% BIBB–hexane solution was poured on the top surface of the membrane and left for 1 minute to immobilize the brominated initiator. Finally, ATRP was conducted by using 1.81 wt% MEA in a methanol solvent and adding 0.35 g of ascorbic acid, 0.02 g of $CuBr_2$ and 0.06 g of TPMA. The ATRP reaction was conducted at room temperature, and the reaction time ranged from 5 min to 48 h. The MEA-treated membranes were thoroughly washed with pure water, followed by storage in the refrigerator. Prior to being subjected to the ATRP reaction, the membranes were precisely cut to a diameter of 37 mm for use in membrane performance evaluation tests and a diameter of 10 mm for use in surface characterization.

2.3. Characterization of the membranes modified with PMEA

The 10 mm diameter modified membranes were vacuum-dried at 30 °C for 30 min. Next, each membrane was weighed thrice to ensure the grafting amount was determined precisely. The grafting amount indicates the degree of grafting and was calculated with:

$$\text{Grafting amount}\ \left[\text{mg cm}^{-2}\right] = \frac{(W - W_0)\ [\text{mg}]}{A\ [\text{cm}^2]} \quad (1)$$

where W and W_0 represent the weight of the membranes after and before ATRP, respectively, and A represents the membrane area.

SEM (JCM-7000; JEOL, Japan) was used to observe the surface structure. The surface chemical composition was determined *via* ATR-FTIR (FT/IR-4200; JASCO Corporation, Japan). The zeta potential of the membrane surface was analyzed using a zeta potential and particle size analyzer (ELSZ-2KH, Otsuka Electronics Co., Ltd., Japan).

2.4. Evaluation of the membrane performance

2.4.1. Pure water permeability and salt rejection. The membrane performance was evaluated using the customized setup shown in Fig. 1. The effective membrane area was 8.0 cm^2, the temperature was 25 ± 0.5 °C, the flow rate was 9.9 mL min^{-1} and the magnetic stirrer was operated at 500 rpm. The pure water permeability (L_p) was determined using deionized water as the feed, and the salt rejection was determined using a 500 ppm NaCl solution. The NaCl concentration of the feed and permeate was measured with an electrical conductivity meter. The grafting amounts of the membranes used for these evaluations with ATR-FTIR and the zeta potential measurements described in section 2.3. were 0 (unmodified), 0.052, 0.062, 0.068, 0.14 and 0.23 mg cm^{-2}.

2.4.2. Filtration tests. First, pure water was supplied using the same apparatus. The flow rate was kept at 0.70 mL min^{-1}, and the applied pressure was controlled to achieve a pure water flux of 1.0 m^3 m^{-2} per day (corresponding to 1.16×10^{-5} m^3 m^{-2} s^{-1} or 0.56 mL min^{-1} for the system). The feed solution was then changed to an aqueous solution containing 10 ppm lysozyme, guar gum or TEGMO. To guarantee 80% recovery, the pressure was adjusted to achieve a flux of 1.16×10^{-5} m^3 m^{-2} s^{-1} after each flux measurement made at 2, 5, 24 and 48 h. The normalized flux (J_{norm}, as defined below) was examined with time to evaluate the effectiveness of surface modification with PMEA:

$$J_{norm} = J_{real} \times \frac{0.75}{\Delta P_{real}} \tag{2}$$

where J_{real} denotes the experimentally obtained flux and ΔP_{real} denotes the transmembrane pressure before tuning. The value of J_{norm} corresponds to the flux achieved at ΔP = 0.75 MPa. A decrease in J_{norm} indicates membrane fouling. Thus, J_{norm} can be used to quantitatively assess the membrane performance. The membranes used for the tests are summarized in Table 1. We confirmed that the solutes (lysozyme, guar gum and TEGMO) were completely rejected in all the experiments.

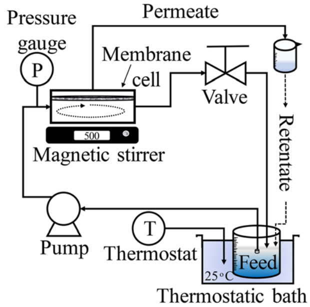

Fig. 1 Schematic of the apparatus used to evaluate the membrane performance.

2.4.3. Contact tests. Contact tests were performed to assess how adsorption of the organic foulants increased the filtration resistance. The contact test method was initially developed for microfiltration membranes[37] and was adapted to RO membranes for the first time in this study. A concentration polarization model was employed to estimate the solute concentration at the surface of the membrane during the filtration tests described in section 2.4.2. Aqueous solutions of the solutes at the estimated concentrations were then prepared. The membrane was mounted on a cell, and the membrane cell (with the permeation side sealed) was allowed to come in contact with an aqueous solution for 48 h over a magnetic stirrer set to 500 rpm. Subsequently, the membrane and the cell were rinsed with pure water. The membrane performance recovery was then evaluated from the pure water permeability and flux variation over time. The results provided clear evidence of the contribution of the adsorption of each foulant to the reduction in the filtrate flux during the filtration test.

The foulant concentration at the surface of the membrane mounted on the cell was estimated using a mass transfer coefficient that was estimated using the following empirical equation (obtained by the osmotic pressure method):[38,39]

$$\frac{C_m - C_p}{C_b - C_p} = \exp\left(\frac{J_v}{k}\right) \tag{3}$$

$$k = 16 \times \left(\frac{v}{D}\right)^{0.44} \times \left(\frac{u}{v}\right)^{0.3} \times D \tag{4}$$

$$D = 8.76 \times 10^{-9} \times (M_w)^{-0.48} \tag{5}$$

$$u = \frac{16\pi\omega}{1000} \times \frac{1}{60} \tag{6}$$

where C_b, C_p and C_m [ppm] denote the foulant concentration of the bulk, permeate and membrane surface, respectively; J_v [m^3 m^{-2} s^{-1}] denotes the flux; k [m s^{-1}] denotes the mass transfer coefficient; v [m^2 s^{-1}] denotes the kinetic viscosity; D [m^2 s^{-1}] denotes the diffusion coefficient; M_w [g mol^{-1}] denotes the molecular weight; u [m s^{-1}] denotes the velocity of the membrane cell and ω [rpm] denotes the rotation speed of the magnetic stirring bar.

3. Results and discussion

3.1. Impact of the polymerization time on the grafting amount

Fig. 2 shows that the grafting amount increased with the polymerization time because extending the reaction time allowed the polymer chains to grow. As the reaction time

Table 1 Membranes used for the filtration tests and the contact tests

Foulant	Membranes for filtration test [mg cm^{-2}]	Membranes for contact test [mg cm^{-2}]	Figure
Lysozyme	0, 0.025, 0.038, 0.043, 0.061	0.04	Fig. 7
Guar gum	0, 0.038, 0.040, 0.042, 0.052	0.04	Fig. 8
TEGMO	0, 0.023, 0.024	0.04	Fig. 9

increased, more polymerization occurred and the grafting amount increased. It ranged widely from 0.020 to 0.23 mg cm^{-2}.

3.2. Membrane characterization

Fig. 3 shows the pictures of the surface of (a) a pristine membrane, (b) the modified membranes with a grafting amount of 0.04 mg cm^{-2}, and (c) that of 0.08 mg cm^{-2}, which were taken by SEM. No clear difference was observed between the pristine membrane and the modified membranes, indicating that the membrane was not damaged at all by the grafting procedure. Fig. 4(a) shows the results of the ATR-FTIR analysis conducted on a pristine membrane and a modified membrane whose grafting amount was 0.15 mg cm^{-2}. A peak at 1660 cm^{-1} appears in the spectra of both membranes, which corresponds to the amide I band and is characteristic for polyamide-based RO membranes. The peak at approximately 1730 cm^{-1} appears only in the spectrum of the modified membrane and corresponds to the C═O stretching vibration of PMEA. The peak intensity generally increases with the grafting amount. Fig. 4(b) shows that the ratio of the PMEA peak to the polyamide peak (I^{1730}/I^{1660}) is positively correlated with the grafting amount. Taken together with the findings in Fig. 2, these results indicate that the peak ratio increased with the polymerization time. Theoretically, the grafting was expected to be performed uniformly because the polymerization step was a rate-determining step in ATRP. The diffusion of the MEA monomer cannot be a rate-determining step. In fact, the concentration of MEA was as high as 1.81 wt% in this study.

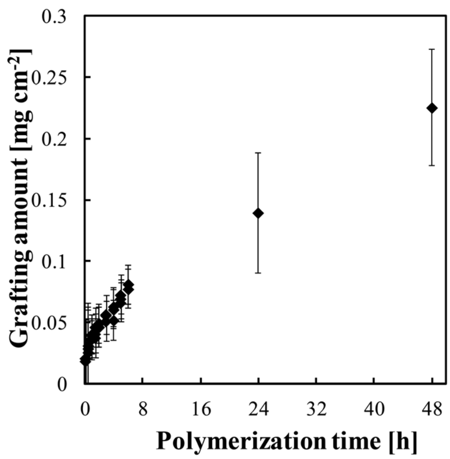

Fig. 2 Relationship between the polymerization time and the grafting amount.

Fig. 5 shows the zeta potential of the surface of the modified membrane in response to the grafting amount. The pristine membrane carried negative charges of up to −26 mV. The charge of the surface grafted with PMEA was less negative, indicating that the grafting process was successful. The negative charge approached neutrality with increasing grafting amount. One contributing factor to this phenomenon was the shielding effect of the grafted polymers, which decreased the exposure of the carboxyl groups on the surface of the polyamide layer. This trend in the zeta potential aligns with the observation of the zeta potential of microfiltration membranes becoming neutral with increasing PMEA grafting amount.[40]

3.3. Impact of the grafting amount on the pure water permeability and salt rejection

Fig. 6(a) illustrates the relationship between the grafting amount and L_p. Membranes with higher grafting amounts exhibited lower L_p values, resulting in the downward trend in the figure. For instance, compared with the L_p of the pristine membrane, the L_p of the membranes whose grafting amounts were 0.052 mg cm^{-2} and 0.23 mg cm^{-2} was lower by 2.7% and 84%, respectively. There was a relatively slight decrease in L_p for membranes whose grafting amounts were smaller than 0.05 mg cm^{-2}. Higher grafting amounts resulted in a more substantial reduction in L_p, which is mainly attributed to the formation of a thick PMEA layer on the membrane surface. Fig. 6(b) shows the relationship between the grafting amount and the observed rejection of NaCl. All the modified membranes exhibited similar salt rejection, which ranged from 97% to 98% at a transmembrane pressure of 1.2 MPa. This result further demonstrates that PMEA did not affect the membrane performance adversely. The consistent and high salt rejection observed across all the modified membranes demonstrates the effectiveness of the ATRP method for introducing PMEA onto the membrane surface without compromising the desalination performance.

3.4. Low-fouling properties

3.4.1. Lysozyme fouling. To compare the performance of membranes with different grafting amounts, the variation in the normalized flux for lysozyme (the model protein-like foulant) is shown in Fig. 7(a). The normalized fluxes corresponding to grafting amounts of 0.025, 0.038 and 0.043 mg cm^{-2} were higher than that for the pristine membrane. This result can be attributed to PMEA endowing the membrane with low-fouling properties while maintaining relatively high pure water permeability. In

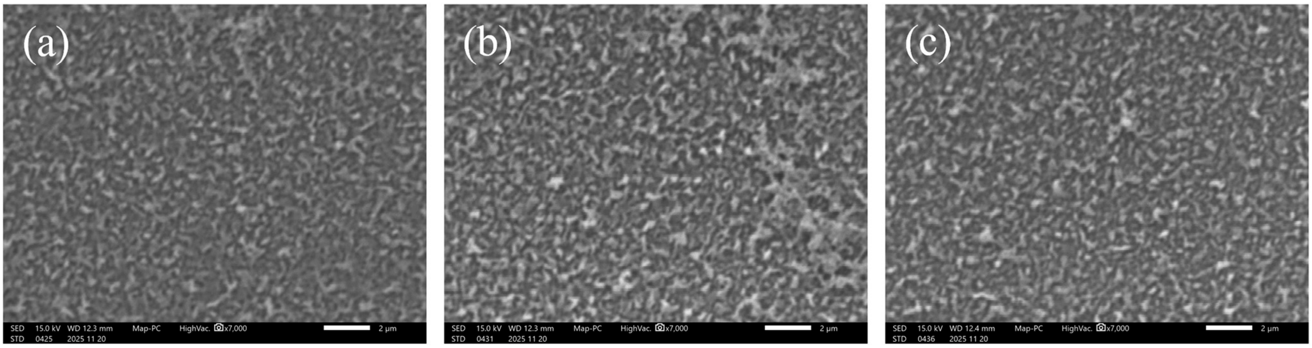

Fig. 3 SEM pictures on the surface of (a) the pristine membrane, (b) the modified membrane with a grafting amount of 0.04 mg cm^{-2} and (c) that of 0.08 mg cm^{-2}. All scale bars represent 2 μm. Magnification: ×7000.

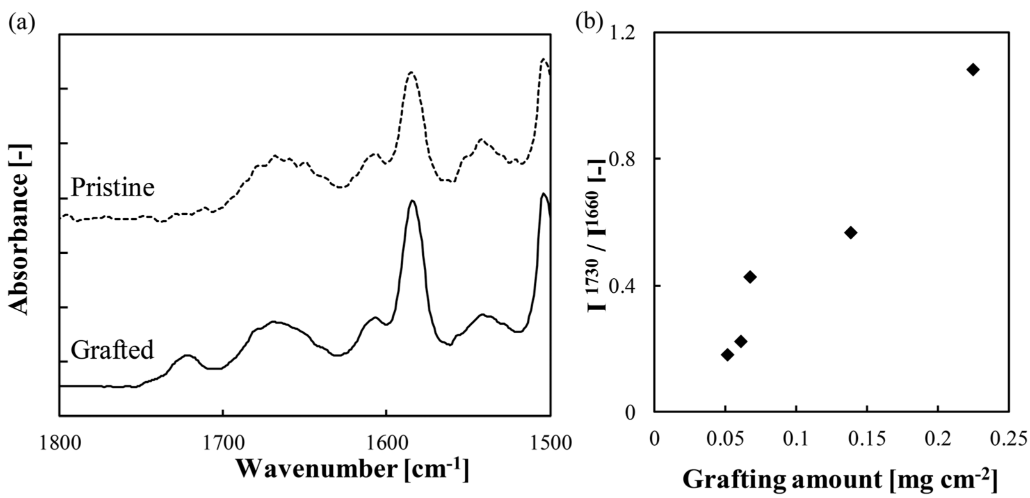

Fig. 4 (a) Attenuated total reflectance Fourier-transform infrared (ATR-FTIR) spectra of the pristine membrane and the membrane grafted with 0.15 mg cm^{-2} poly(2-methoxyethyl acrylate) (PMEA); (b) the peak ratio I^{1730}/I^{1660} *versus* the grafting amount.

contrast, the membrane with a grafting amount of 0.061 mg cm^{-2} had a lower normalized flux than that of the pristine membrane. Although this membrane was low-fouling, the pure water permeability was smaller than that of the pristine membrane, which decreased the normalized flux. These results show that modified membranes with certain grafting amounts had less severe flux reduction when exposed to the lysozyme solution than that of the pristine membrane. Thus, modification with PMEA effectively mitigates fouling by lysozyme, enhancing water permeation. Fig. 7(b) shows how the time-dependent flux changed during pure water permeation tests upon contacting the surfaces of both the pristine and the modified membranes (0.04 mg cm^{-2}) with an aqueous 400 ppm lysozyme solution. This concentration corresponded to that estimated at the membrane surface for the filtration tests shown in Fig. 7(a) conducted using a 10 ppm lysozyme solution. Clearly, the flux of both membranes recovered slightly during the early stage, where the modified membrane with a grafting amount of 0.04 mg cm^{-2} had a higher flux than that of the pristine membrane. This result suggests that the PMEA on the top surface of the modified membrane inhibited the adsorption of lysozyme to the membrane surface. Thus, the low-fouling properties of the modified membrane resulted from the successful suppression of protein adsorption on the membrane surface.

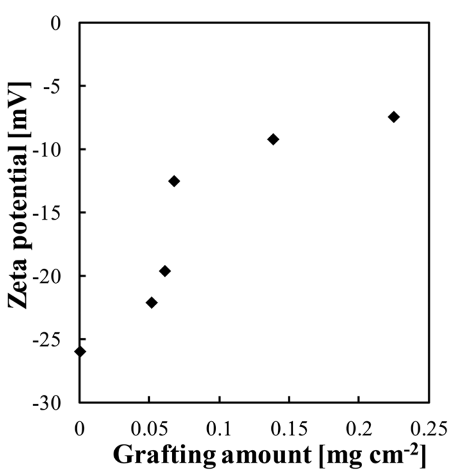

Fig. 5 Relationship between the grafting amount and the zeta potential.

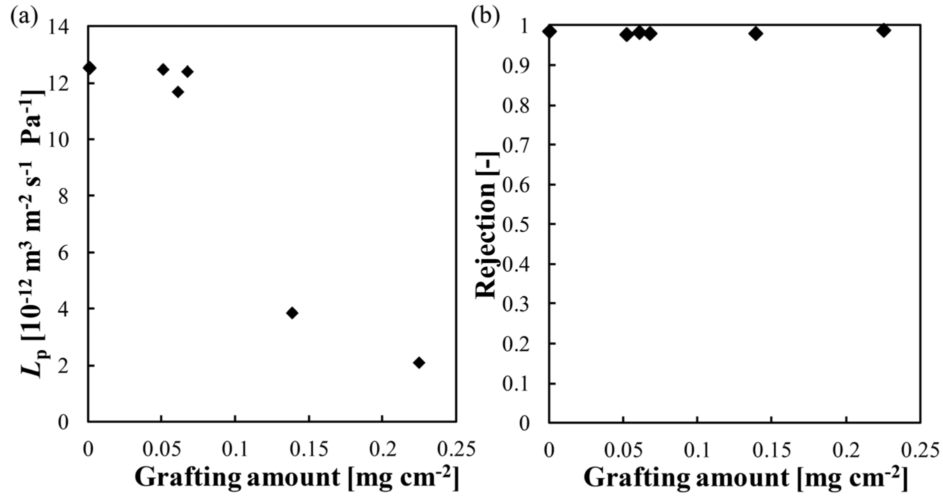

Fig. 6 Relationship between the grafting amount and (a) pure water permeability and (b) observed rejection of NaCl.

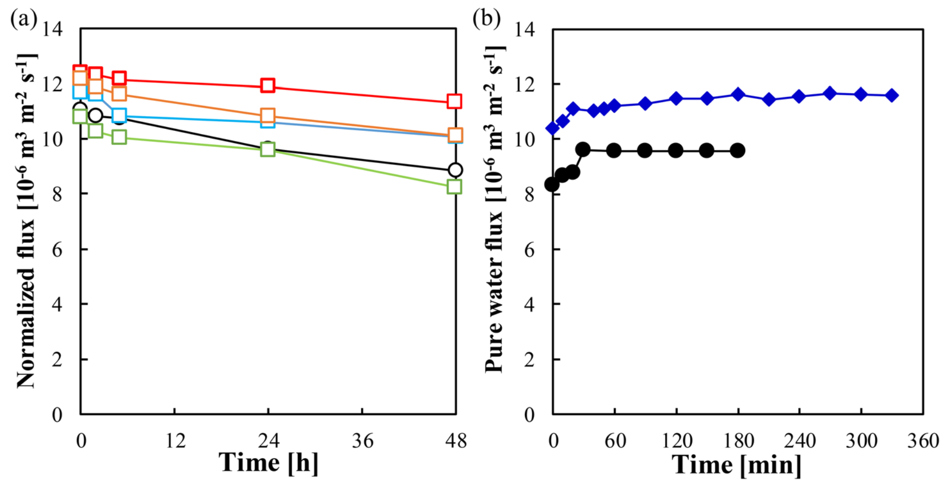

Fig. 7 (a) Time-dependent normalized flux through membranes exposed to a 10 ppm lysozyme solution (○ pristine membrane and membranes with grafting amounts of □ (red) 0.025 mg cm^{-2}, □ (light blue) 0.038 mg cm^{-2}, □ (orange) 0.043 mg cm^{-2} and □ (yellow-green) 0.061 mg $^{-2}$); (b) pure water flux recovery after contacting membranes with a 400 ppm lysozyme solution (● pristine membrane and ◆ a modified membrane with a grafting amount of 0.04 mg cm^{-2}).

3.4.2. Guar gum fouling. Fig. 8(a) shows the variation in the normalized flux for guar gum (the model polysaccharide-like foulant). The normalized flux for the pristine membrane decreased drastically with time because of severe fouling. The results for the membrane with grafting amounts of 0.038, 0.040, 0.042 and 0.052 mg cm^{-2} demonstrate that the introduction of PMEA strongly influenced the fouling of the membrane surface by polysaccharides. Thus, the modified membranes with these specific grafting amounts exhibited less severe flux reduction when exposed to guar gum solution than the pristine membranes. This result highlights the effectiveness of PMEA modification in mitigating fouling caused by guar gum and, thereby, flux reduction. Fig. 8(b) shows how the flux changed with time during pure water permeation tests upon contacting the surfaces of both the pristine and the modified membranes (0.04 mg cm^{-2}) with an aqueous solution containing 1200 ppm guar gum. This concentration corresponded to that estimated at the membrane surface during the filtration tests shown in Fig. 8(a) conducted using a 10 ppm guar gum solution. The PMEA-polymerized membrane had a slightly higher flux than that of the pristine membrane. These results indicate the successful suppression of guar gum adsorption on the modified membrane surface.

3.4.3. TEGMO fouling. Fig. 9(a) shows the variation in the normalized flux for TEGMO (the model surfactant-like foulant). The introduction of PMEA at grafting amounts of 0.023 and 0.024 mg cm^{-2} considerably affected the fouling of the membrane surface by TEGMO. The flux reduction over time for the modified membranes with these grafting amounts was less severe than that for the pristine membranes. This result suggests that PMEA modification effectively mitigated fouling by TEGMO and, thereby, flux reduction. Fig. 9(b) shows how the flux changed over time during pure water permeation tests upon contacting the

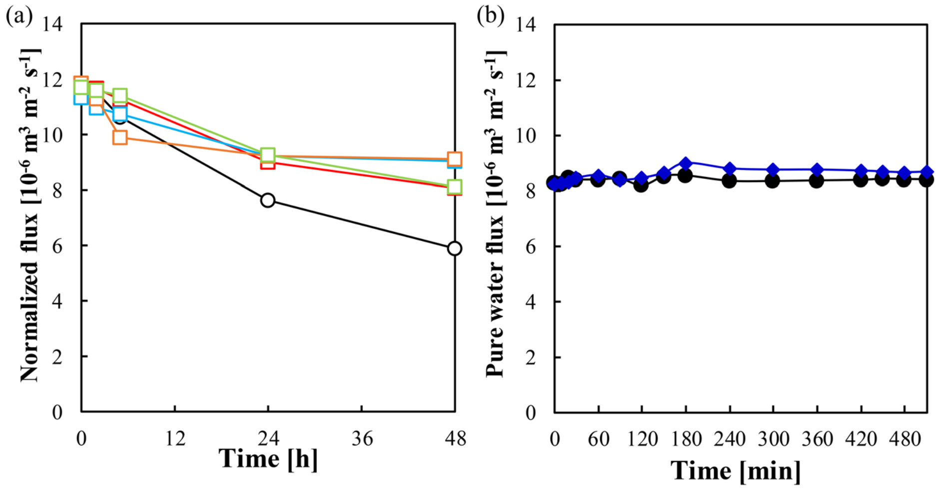

Fig. 8 (a) Time-dependent normalized flux of membranes exposed to a 10 ppm guar gum solution (○ pristine membrane and membranes with grafting amounts of □ (red) 0.038 mg cm^{-2}, □ (light blue) 0.040 mg cm^{-2}, □ (orange) 0.042 mg cm^{-2} and □ (yellow-green) 0.052 mg cm^{-2}); (b) pure water flux recovery of membranes after immersion in a 1200 ppm guar gum solution (● pristine membrane and ◆ a modified membrane with a grafting amount of 0.04 mg cm^{-2}).

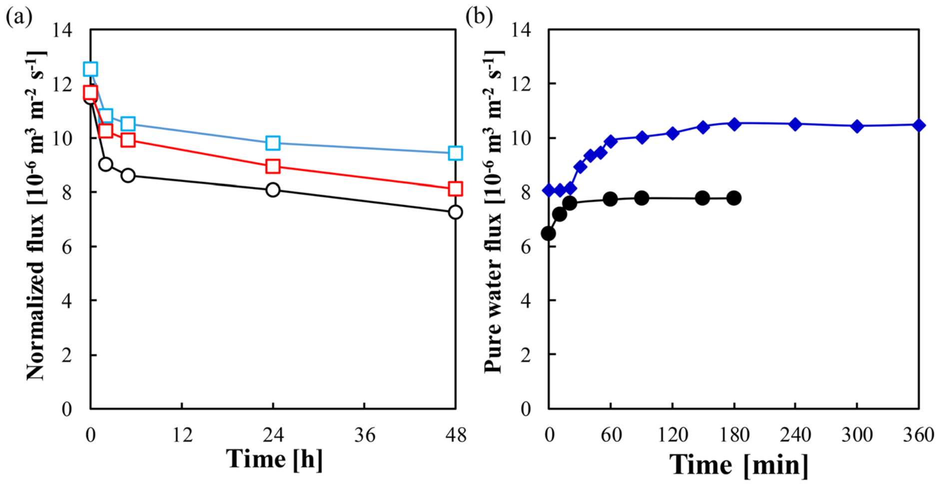

Fig. 9 (a) Time-dependent normalized flux of membranes exposed to a 10 ppm tetraethylene glycol monooctyl ether (TEGMO) solution (○ pristine membrane and membranes with grafting amounts of □ (red) 0.023 mg cm^{-2} and □ (light blue) 0.024 mg cm^{-2}); (b) pure water flux recovery of membranes after immersion in a 110 ppm TEGMO solution (● pristine membrane and ◆ a modified membrane with a grafting amount of 0.04 mg cm^{-2}).

surfaces of both the pristine and the modified membranes (0.04 mg cm^{-2}) with an aqueous 110 ppm TEGMO solution (this concentration corresponded to that estimated at the membrane surface during the filtration tests shown in Fig. 9(a) conducted using a 10 ppm TEGMO solution). The flux through the PMEA-polymerized membrane was clearly higher than that of the pristine membrane. These results indicate successful suppression of TEGMO adsorption on the modified membrane surface.

These findings lead us to conclude that the optimum PMEA grafting amount for ES20 to achieve the desired performance ranged from 0.02 to 0.04 mg cm^{-2}. Within this range, there was a small reduction in the pure water permeability, the salt rejection performance was maintained, and low fouling by proteins, polysaccharides and surfactants was achieved.

4. Conclusion

The feasibility of surface modification of ES20 with PMEA to achieve low-fouling characteristics was demonstrated in this study. First, we used SI-ATRP to indicate that PMEA was successfully grafted on the ES20 surface and confirmed the results through ATR-FTIR and zeta potential measurements. The grafting amount could be tuned by varying the polymerization time, and the surface became more neutral as the grafting amount increased. The grafted PMEA created permeation resistance in the membrane, such that the pure water permeability decreased with the grafting amount. However, the reduction in the pure water permeability was small for grafting amounts below 0.05 mg cm^{-2}. The salt rejection performance was independent of the grafting amount and remained high for the modified membranes. Importantly, the modified membranes with grafting amounts below 0.04 mg cm^{-2} exhibited excellent resistance to fouling by lysozyme, guar gum and TEGMO, suggesting successful suppression of fouling by potential foulants. These achievements will contribute to developing effective strategies for mitigating fouling in low-pressure RO membranes.

Conflicts of interest

The authors declare that they have no known competing financial interests or personal relationships that could have appeared to influence the work reported in this paper.

Data availability

Data will be made available on request.

Acknowledgements

We thank Edanz (https://jp.edanz.com/english-editing-c) for editing a draft of this manuscript.

References

1 C. He, Z. Liu, J. Wu, X. Pan, Z. Fang, J. Li and B. A. Bryan, Future global urban water scarcity and potential solutions, *Nat. Commun.*, 2021, **12**, 4667, DOI: 10.1038/s41467-021-25026-3.

2 H. Shemer, S. Wald and R. Semiat, Future global urban water scarcity and potential solutions, *Membranes*, 2023, **13**, 612, DOI: 10.3390/membranes13060612.

3 W. Musie and G. Gonfa, Fresh water resource, scarcity, water salinity challenges and possible remedies: A review, *Heliyon*, 2023, **9**, e18685, DOI: 10.1016/j.heliyon.2023.e18685.

4 D. L. Zhao, S. Japip, Y. Zhang, M. Weber, C. Maletzko and T.-S. Chung, Emerging thin-film nanocomposite (TFN) membranes for reverse osmosis: A review, *Water Res.*, 2020, **173**, 115557, DOI: 10.1016/j.watres.2020.115557.

5 W. J. Lau, S. Gray, T. Matsuura, D. Emadzadeh, J. P. Chen and A. F. Ismail, A review on polyamide thin film nanocomposite (TFN) membranes: History, applications, challenges and approaches, *Water Res.*, 2015, **80**, 306–324, DOI: 10.1016/j.watres.2015.04.037.

6 Z. Yang, H. Guo and C. Y. Tang, The upper bound of thin-film composite (TFC) polyamide membranes for desalination, *J. Membr. Sci.*, 2019, **590**, 117297, DOI: 10.1016/j.memsci.2019.117297.

7 Y. J. Lim, K. Goh, M. Kurihara and R. Wang, Seawater desalination by reverse osmosis: Current development and future challenges in membrane fabrication – A review, *J. Membr. Sci.*, 2021, **629**, 119292, DOI: 10.1016/j.memsci.2021.119292.

8 K. Park, J. Kim, D. R. Yang and S. Hong, Towards a low-energy seawater reverse osmosis desalination plant: A review and theoretical analysis for future directions, *J. Membr. Sci.*, 2020, **595**, 117607, DOI: 10.1016/j.memsci.2019.117607.

9 S. Habib and S. T. Weinman, A review on the synthesis of fully aromatic polyamide reverse osmosis membranes, *Desalination*, 2021, **502**, 114939, DOI: 10.1016/j.desal.2021.114939.

10 T. Wang, L. Dai, Q. Zhang, A. Li and S. Zhang, Effects of acyl chloride monomer functionality on the properties of polyamide reverse osmosis (RO) membrane, *J. Membr. Sci.*, 2013, **440**, 48–57, DOI: 10.1016/j.memsci.2013.03.066.

11 M. Qasim, M. Badrelzaman, N. N. Darwish, N. A. Darwish and N. Hilal, Reverse osmosis desalination: A state-of-the-art review, *Desalination*, 2019, **459**, 59–104, DOI: 10.1016/j.desal.2019.02.008.

12 G. Kang and Y. Cao, Development of antifouling reverse osmosis membranes for water treatment: A review, *Water Res.*, 2012, **46**, 584–600, DOI: 10.1016/j.watres.2011.11.041.

13 W. S. Ang, N. Y. Yip, A. Tiraferri and M. Elimelech, Chemical cleaning of RO membranes fouled by wastewater effluent: Achieving higher efficiency with dual-step cleaning, *J. Membr. Sci.*, 2011, **382**, 100–106, DOI: 10.1016/j.memsci.2011.07.047.

14 A. E. Contreras, Z. Steiner, J. Miao, R. Kasher and Q. Li, Studying the Role of Common Membrane Surface Functionalities on Adsorption and Cleaning of Organic Foulants Using QCM-D, *Environ. Sci. Technol.*, 2011, **45**, 6309–6315, DOI: 10.1021/es200570t.

15 J. Wu, Z. Wang, Y. Wang, W. Yan, J. Wang and S. Wang, Polyvinylamine-grafted polyamide reverse osmosis membrane with improved antifouling property, *J. Membr. Sci.*, 2015, **495**, 1–13, DOI: 10.1016/j.memsci.2015.08.007.

16 W. S. Ang, A. Tiraferri, K. L. Chen and M. Elimelech, Fouling and cleaning of RO membranes fouled by mixtures of organic foulants simulating wastewater effluent, *J. Membr. Sci.*, 2011, **376**, 196–206, DOI: 10.1016/j.memsci.2011.04.020.

17 Y.-Q. Xu, Y.-H. Wu, X. Tong, L.-W. Luo and H.-B. Wang, How to select ideal model organic matters for membrane fouling research on water and wastewater treatment, *Water Cycle*, 2023, **4**, 55–59, DOI: 10.1016/j.watcyc.2023.02.002.

18 V. Freger, J. Gilron and S. Belfer, TFC polyamide membranes modified by grafting of hydrophilic polymers: an FT-IR/AFM/TEM study, *J. Membr. Sci.*, 2002, **209**, 283–292, DOI: 10.1016/S0376-7388(02)00356-3.

19 Y. Guan, S.-L. Li, Z. Fu, Y. Qin, J. Wang, G. Gong and Y. Hu, Preparation of antifouling TFC RO membranes by facile grafting zwitterionic polymer PEI-CA, *Desalination*, 2022, **539**, 115972, DOI: 10.1016/j.desal.2022.115972.

20 M. Liu, Q. Chen, L. Wang, S. Yu and C. Gao, Improving fouling resistance and chlorine stability of aromatic polyamide thin-film composite RO membrane by surface grafting of polyvinyl alcohol (PVA), *Desalination*, 2022, **539**, 115972, DOI: 10.1016/j.desal.2015.03.028.

21 N. S. Kandiyote, T. Avisdris, C. J. Arnusch and R. Kasher, Grafted Polymer Coatings Enhance Fouling Inhibition by an Antimicrobial Peptide on Reverse Osmosis Membranes, *Langmuir*, 2019, **35**, 1935–1943, DOI: 10.1021/acs.langmuir.8b03851.

22 J. Gao, J. Liu, L. Liu, J. Dong, X. Zhao and J. Pan, Multiple Interface Reactions Enabled Zwitterionic Polyamide Composite Reverse Osmosis Membrane for Enhanced Permeability and Antifouling Property, *Ind. Eng. Chem. Res.*, 2023, **62**, 2904–2912, DOI: 10.1021/acs.iecr.2c04058.

23 Z. Yang, D. Saeki and H. Matsuyama, Zwitterionic polymer modification of polyamide reverse-osmosis membranes via surface amination and atom transfer radical polymerization for anti-biofouling, *J. Membr. Sci.*, 2018, **550**, 332–339, DOI: 10.1016/j.memsci.2018.01.001.

24 H. Z. Shafi, Z. Khan, R. Yang and K. K. Gleason, Surface modification of reverse osmosis membranes with zwitterionic coating for improved resistance to fouling, *Desalination*, 2015, **362**, 93–103, DOI: 10.1016/j.desal.2015.02.009.

25 D. Saeki, T. Tanimoto and H. Matsuyama, Anti-biofouling of polyamide reverse osmosis membranes using phosphorylcholine polymer grafted by surface-initiated atom transfer radical polymerization, *Desalination*, 2014, **350**, 21–27, DOI: 10.1016/j.desal.2014.07.004.

26 K. Akamatsu, T. Furue, F. Han and S. Nakao, Plasma graft polymerization to develop low-fouling membranes grafted with poly(2-methoxyethylacrylate), *Sep. Purif. Technol.*, 2013, **102**, 157–162, DOI: 10.1016/j.seppur.2012.10.013.

27 K. Akamatsu, T. Saito, H. Ohashi, X. Wang and S. Nakao, Plasma Graft Polymerization and Surface-Initiated Atom Transfer Radical Polymerization: Characteristics of Low-Fouling Membranes Obtained by Surface Modification with Poly(2-methoxyethyl Acrylate), *Ind. Eng. Chem. Res.*, 2021, **60**, 15248–15255, DOI: 10.1021/acs.iecr.1c02462.

28 K. Akamatsu, M. Sano, F. Okada, S. Nakao and X. Wang, Immersion in advanced oxidation water followed by AGET-ATRP to develop low-fouling microfiltration membranes by grafting poly(2-methoxyethyl acrylate), *Ind. Eng. Chem. Res.*, 2023, **62**, 10611–10618, DOI: 10.1021/acs.iecr.3c01571.

29 M. Tanaka, T. Motomura, M. Kawada, T. Anzai, Y. Kasori, T. Shiroya, K. Shimura, M. Onishi and A. Mochizuki, Blood compatible aspects of poly(2-methoxyethylacrylate) (PMEA)—relationship between protein adsorption and platelet adhesion on PMEA surface, *Biomaterials*, 2020, **21**, 1471–1481, DOI: 10.1016/S0142-9612(00)00031-4.

30 M. Tanaka, T. Motomura, N. Ishii, K. Shimura, M. Onishi, A. Mochizuki and T. Hatakeyama, Cold crystallization of water in hydrated poly(2-methoxyethyl acrylate) (PMEA), *Polym. Int.*, 2000, **49**, 1709–1713, DOI: 10.1002/1097-0126(200012)49:12<1709::AID-PI601>3.0.CO;2-L.

31 M. Tanaka, S. Kobayashi, D. Murakami, F. Aratsu, A. Kashiwazaki, T. Hoshiba and K. Fukushima, Design of Polymeric Biomaterials: The "Intermediate Water Concept", *Bull. Chem. Soc. Jpn.*, 2019, **92**, 2043–2057, DOI: 10.1246/bcsj.20190274.

32 K. Sato, S. Kobayashi, M. Kusakari, S. Watahiki, M. Oikawa, T. Hoshiba and M. Tanaka, The Relationship Between Water Structure and Blood Compatibility in Poly(2-methoxyethyl Acrylate) (PMEA) Analogues, *Macromol. Biosci.*, 2015, **15**, 1296–1303, DOI: 10.1002/mabi.201500078.

33 R. Nagumo, K. Akamatsu, R. Miura, A. Suzuki, N. Hatakeyama, H. Takaba and A. Miyamoto, A Theoretical Design of Surface Modifiers for Suppression of Membrane Fouling: Potential of Poly(2-mehoxyethylacrylate), *J. Chem. Eng. Jpn.*, 2012, **45**, 568–570, DOI: 10.1252/jcej.12we110.

34 Y. Zhang, Z. Wang, W. Lin, H. Sun, L. Wu and S. Chen, A facile method for polyamide membrane modification by poly(sulfobetaine methacrylate) to improve fouling resistance, *J. Membr. Sci.*, 2013, **446**, 164–170, DOI: 10.1016/j.memsci.2013.06.013.

35 A. J. Blok, R. Chhasatia, J. Dilag and A. V. Ellis, Surface initiated polydopamine grafted poly([2-(methacryoyloxy)ethyl]trimethylammonium chloride) coatings to produce reverse osmosis desalination membranes with anti-biofouling properties, *J. Membr. Sci.*, 2014, **468**, 216–223, DOI: 10.1016/j.memsci.2014.06.008.

36 U. Hirsch, M. Ruehl, N. Teuscher and A. Heilmann, Antifouling coatings via plasma polymerization and atom transfer radical polymerization on thin film composite membranes for reverse osmosis, *Appl. Surf. Sci.*, 2018, **436**, 207–216, DOI: 10.1016/j.apsusc.2017.12.038.

37 S. Ohno, S. Nakao, X. Wang and K. Akamatsu, Morphology and Surface Characteristics of PVDF/Poly(2-methoxyethyl acrylate) Blend Membranes Prepared via NIPS and Their pH-Independent Low-Fouling Properties, *Ind. Eng. Chem. Res.*, 2022, **61**, 15326–15335, DOI: 10.1021/acs.iecr.2c02271.

38 G. Jonsson, Boundary layer phenomena during ultrafiltration of dextran and whey protein solutions, *Desalination*, 1984, **51**, 61–77, DOI: 10.1016/0011-9164(84)85053-5.

39 G. B. van den Berg, I. G. Rácz and C. A. Smolders, Mass transfer coefficients in cross-flow ultrafiltration, *J. Membr. Sci.*, 1989, **47**, 25–51, DOI: 10.1016/S0376-7388(00)80858-3.

40 K. Akamatsu, M. Sano, F. Okada, S. Nakao and X. Wang, Poly(2-methoxyethyl acrylate)-grafted microfiltration membranes exhibiting low-fouling properties in the presence of salt species, *RSC Appl. Interfaces*, 2024, **1**, 677–683, DOI: 10.1039/D4LF00129J.